Interactive Volume Manipulation for Supporting Preoperative Planning

M. Nakao, S. Yano, T. Matsuyuki, T. Kawamoto and K. Minato
Grad. Sch. of Information Science, Nara Institute of Science and Technology, JAPAN

Abstract. This paper presents a volume manipulation framework by which surgeons can interactively manipulate soft models like through surgical tools. The framework robustly simulates common surgical manipulations such as grasping, holding, cutting and retraction. We simulate cutting based on FEM formulation by replacing vertices and eliminating elements, without subdividing elements or adding new vertices. The size of stiffness matrix is constant. We also present real-time volume shading methods for deformable modeling. Our algorithms achieved interactive response in volume manipulation. Several surgical approaches and procedures were rehearsed and used for preoperative discussion.

Keywords. Volume manipulation, Cutting, Deformation and Preoperative rehearsal

1. Introduction

In light of the difficulties surgeons face in choosing optimal surgical scenarios for their patients, preoperative surgical simulation on volumetrically rendered images from CT/MRI dataset is now regarded as essential for planning and communication between medical staffs. Preoperative rehearsal is a known concept and volume planning systems [1][2] have been proposed. However, most systems were designed for rigid voxel models or interactive soft tissue operation was limited due to modeling complexity, volume rendering cost and lack of manipulation interface.

We develop a volume manipulation framework that allows surgeons to interactively manipulate soft models like through surgical tools (see **Figure 1**). The framework handles both a tetrahedral mesh and CT/MRI volume, and represents volume deformation and cutting based on finite element formulation. This paper mainly introduces two methods: soft tissue modeling for simulating cutting with deformation and a volume visualization algorithm for time-varying deformable models.

For simulating cutting on elastic objects, removal of tetrahedral elements is a simple approach [3]. Since only removal of elements have problems of yielding visual artifacts and of decreasing total volume of the models, topological adaptation is required. One approach for topological update is subdivision of tetrahedral meshes [4][5], which defines incision using newly created small elements. Splitting mesh on the boundary of elements [6][7] is another approach. Combined methods [8] have been recently explored. However, most algorithms for topological change increase their computation cost in progress of cutting manipulation. New tetrahedral elements with bad shape

Corresponding Author: Megumi Nakao, 8916-5 Takayama, Ikoma, Nara, JAPAN. E-mail: meg@is.naist.jp

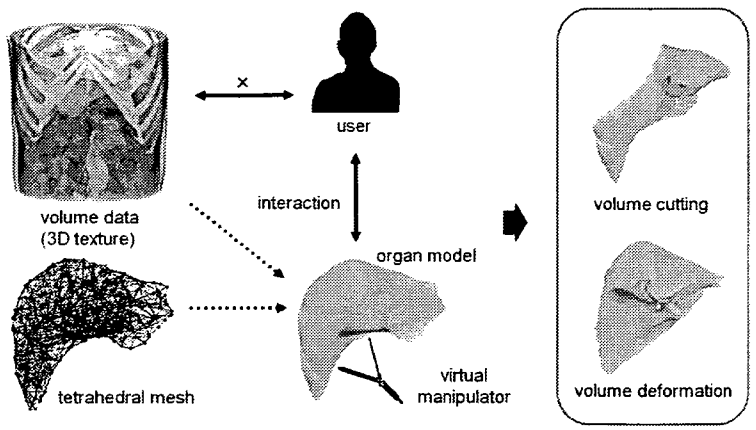

Figure 1. The basic design of our framework. The elastic behavior of organs is physically simulated and volumetrically rendered. Interactive performance is achieved on GPU by not updating volume data.

created through topological update exert a bad influence for stability and accuracy of the simulation. Unlike existing methods, we aim to shape visually valid incision by relocation and constraints of initial vertices. The vertex count is preserved. This approach avoids increase of computation cost and enables fast update of physical status through modifying meshes.

Real-time shading on time-varying, volumetrically rendered objects is also a challenging issue. Gray-level gradient [9] pre-computationally defines gradient voxels from 3D texture. However, since reconstructing voxels takes high computational costs, this approach is not available for interactive volume deformation. Although Correa et al. presented a volume shading algorithm on deformed objects [10], it does not support interactive manipulation. Our approach supports interactive, arbitrary manipulation, and achieves fast volume shading by per-vertex gradient approximation and its interpolation on GPUs.

2. Finite Element based Modeling of Cutting and Deformation

2.1 Vertex-preserving Cutting

When soft tissue is cut in the real world, two facing surfaces (called **cut surfaces**) are created, and the tissue connectivity is broken. The cut surfaces and tiny space between them are physical phenomena with geometrical change that should be simulated. Our interest is what a variety of valid cut surfaces can be configured through only the relocation of vertices, without subdividing the tetrahedral elements nor creating new vertices. This makes it possible to prevent the number of vertices from increasing in cutting procedure, therefore preventing increase in calculation time.

Figure 2 briefly illustrates known methods and our approach using 2D outline of the process. In our approach (d), when a blade path is given, the vertices of the intersected elements are projected onto the path. The two parallel lines (surfaces in the 3D virtual space) composed by relocated vertices are used to shape the cut surfaces. Also, some

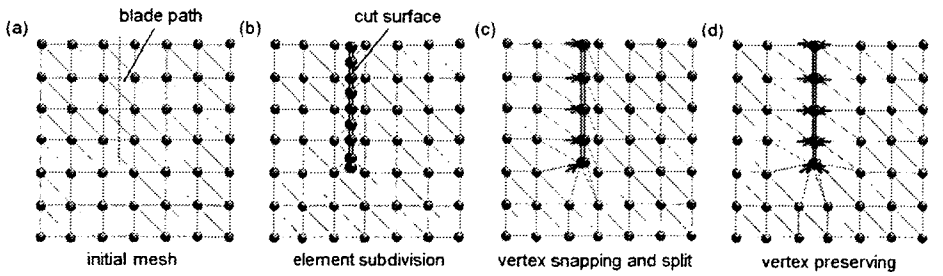

Figure 2. Three modeling methods for soft tissue cutting. Our approach, a vertex preserving cutting method creates cut surfaces using existing vertices and constraints to preserve 3D shape and feature of initial meshes.

vertices are constrained to preserve 3D shape and sharp feature of initial meshes. After the vertices have been relocated, removing elements that intersect the blade path makes it possible to model the tiny space between cut surfaces and simulate the physical behavior of the incision. In the finite element modeling, the stiffness matrix must be updated through relocation of vertices and the elimination of elements. With methods that use element decomposition to represent the cutting process such as (b) and (c), the size of the stiffness matrix increases. However, in our model, the size is constant. We utilize this feature for solving linear equation in finite element formulation, and enable fast cutting simulation with deformation.

When a tetrahedral element is cut, the vertices $\mathbf{v}_i$ of the element are projected onto the blade path. The blade path forms set of surfaces $\mathbf{S}_t$ (t = 0, 1, ...), which are called **sweep surfaces**. Then, the update vector $\Delta\mathbf{v}_i$ is defined as the following equation:

$$\Delta\mathbf{v}_i = \{\mathbf{n}_t \cdot (\mathbf{v}_i - \mathbf{p}_t)\}\mathbf{n}_t \tag{1}$$

where $\mathbf{n}_t$ is the normal vector of the sweep surface $\mathbf{S}_t$. $\mathbf{p}_t$ is an arbitrary point on the $\mathbf{S}_t$. Vertices that are updated outside of sweep surfaces $\mathbf{S}_0, \mathbf{S}_1$ ... generate visual artifact. Therefore, such vertices are again relocated by projecting them onto the boundary of given sweep surfaces. In order to preserve the feature of the initial mesh and to update the vertices fast and definitely, we introduce simple constraints into topology modification.

After the relocation of the vertices, the tetrahedral elements that are collapsed between the cut surfaces are deleted. Then, the stiffness matrix must be updated in the finite element modeling. For all tetrahedra that are deleted or affected by relocation of vertices, the element stiffness matrix $\mathbf{K}_e$ is subtracted from stiffness matrix $\mathbf{K}$ concerned with corresponding vertex. Note that $\mathbf{K}_e$ is pre-computed per tetrahedral element before cutting manipulation.

2.2 Surface-constraint-based Deformation

Other surgical procedures like grasping, holding and exclusion are also handled in our framework. When the intersection between the organ model and the virtual manipulator is detected, the manipulation area is regarded as grasped and forcible displacement is applied to the controlled vertices as a boundary displacement condition in finite element formulation. To simulate the surgical forceps and retractors for the rehearsal of

the surgery in these cases, we constrain the vertices on the constraint surface of the manipulator by displacing the controlled vertices to new positions.

Next, the controlled vertices are geometrically transformed while satisfying the given surface constraint. This allows users to grasp the manipulation area and to work with it interactively, as they would when manipulating actual surgical tools. By translating and rotating the organ, for example, users can directly simulate the maneuvers of excluding or holding as they prepare the surgical workspace for planning of the surgery.

3. Volume Rendering with Shading for Deformable Models

Volume manipulation results can be visualized in real time by volume-rendering the tetrahedral mesh with 3D texture mapping. The process is derived from a method for rendering volumes based on texture mapping techniques [11]. We render tetrahedral elements using the cross sections (called **proxy geometry**). When the vertices are displaced by model deformation, the proxy geometry is updated based on the deformed mesh topology. The initial coordinates of vertices are used as texture coordinates.

In order to perform volume shading, an initial CT/MRI intensity volume, a gradient volume and a tetrahedral mesh are prepared. When displacement is given by mesh deformation, our framework defines rotation matrix **M** per vertex using initial vertices and displaced vertices. We approximate the rotational component around the vertex $\mathbf{v}_i$ by selecting its orthonormal basis. Then, the rotation matrix is interpolated on GPUs. Initial gradient per voxels that are transformed by the interpolated rotation matrix is used for shading. Since this approach does not need update of volume data, fast volume shading can be performed.

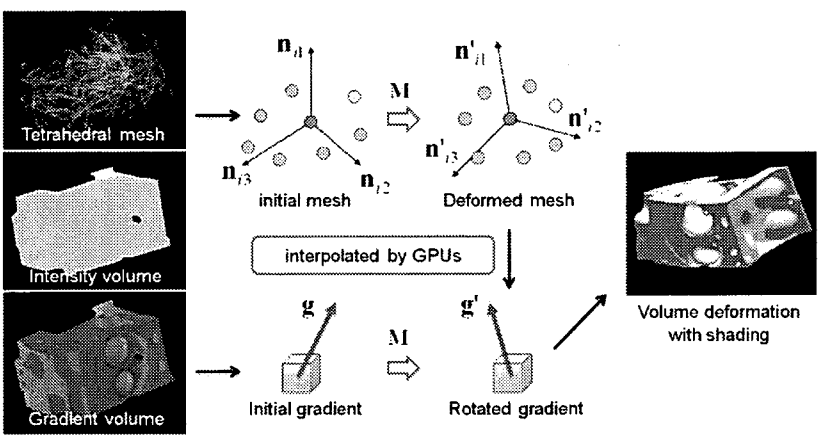

Figure 3. A volume shading algorithm for time-varying deformable models.

4. Results and Discussion

We applied CT volume dataset (volume size: 256^3) to our volume manipulation framework on general purpose PC with Intel Core2Duo 2.93GHz, 2048Mbytes

memory and nVidia GeForce8800 graphic card. **Figure 4** and **5** show its applications. Common surgical manipulation like grasping, holding, cutting and retraction was simulated. The pre-computed Conjugate Gradient algorithm was employed to solve linear large equation in cutting finite element models. **Table 1** shows the refresh rates and model parameters. Interactive manipulation was possible for all datasets. Also, our framework was used for preoperative rehearsal of thoracoscopic surgery based on a patient's CT volume dataset. The volunteer surgeon pinched a part of the lung tissue for clipping the bulla as shown in **Figure 6**. Real surgery videos and volumetrically rendered images demonstrate similar manipulations and surgical views can be preoperatively simulated.

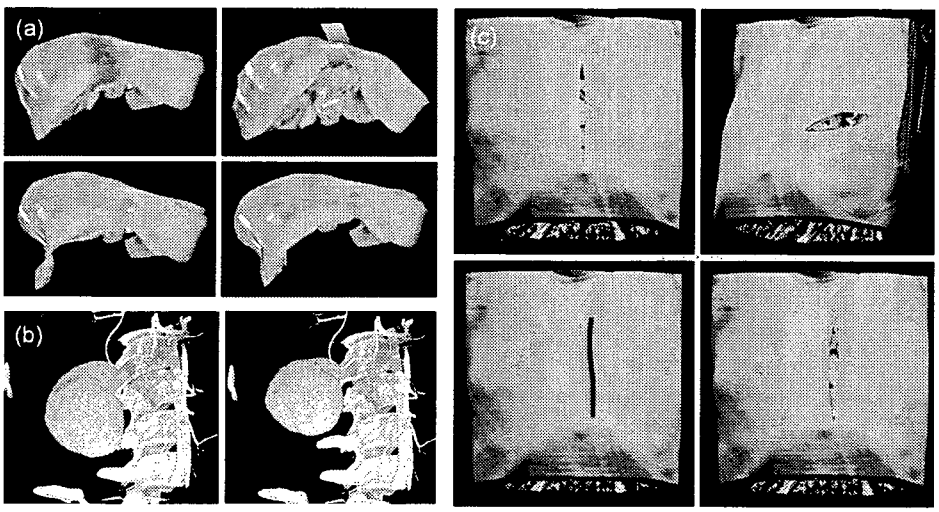

Figure 4. Volume manipulation examples: (a) liver volume deformation by grasping manipulation, (b) kidney rotation and deformation and (c) volume cutting and retraction of incision. The incision can be interactively modified on the rendered image.

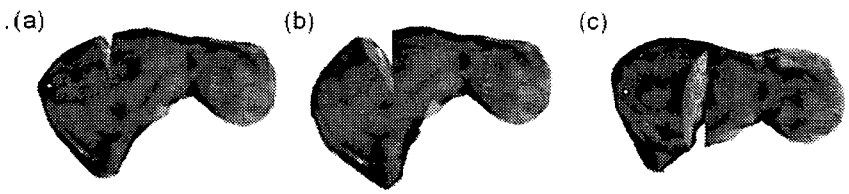

Figure 5. (a) (b) Interactive cutting with holding a part of liver volume model. Internal structure can be observed. (c) Another cut example with different depth and deformation.

Table 1. Refresh rates for overall simulation and rendering.

	Volume size	Vertices	FPS (frame per sec)
Liver	256^3	567	38
Kidney	256^3	424	45
Breast	256^3	613	20
Lung	256^3	344	50

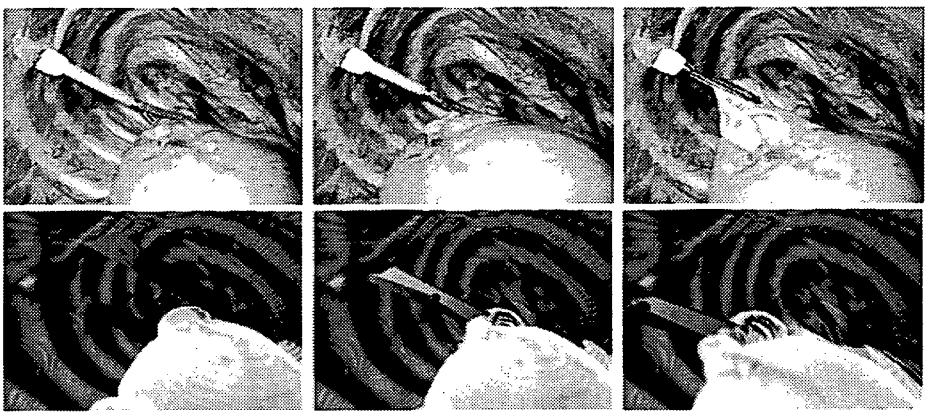

Figure 6. Lung deformation. (a) surgical videos and (b) volume deformation by virtual tools.

5. Conclusion

This paper introduced our volume manipulation framework and presented techniques on vertex-preserving cutting and GPU-based volume shading. We are currently developing an adaptive surgical procedure template and pen-based interface for supporting easy and quick patient-specific preoperative planning.

Acknowledgements

We wish to thank Assistant Professor Koji Yoshimura for preparing clinical dataset and the valuable discussion. This research is supported by Grant-in-Aid for Scientific Research (S) (16100001) and Young Scientists (A) (16680024) from The Ministry of Education, Culture, Sports, Science and Technology, Japan.

References

[1] B. Pflesser, R. Leuwer, U. Tiede, K.H. Hohne, "lanning and Rehearsal of Surgical Interventions in the Volume Model" Stud. Health Tech. Inform. Vol. 70, pp. 259-264, 2000.

[2] H. Takiuchi, Y. Mori, H. Shima, M. Tanooka et al. "Kidney Displacement Simulator for Retroperitoneal Laparoscopic Nephrectomy", J. Urology, Vol. 174, No. 6, pp. 2111-2114, 2005.

[3] C. Forest and H. Delingette and N. Ayache", "Cutting simulation of manifold volumetric meshes", Medical Image Computing and Computer Assisted Intervention(MICCAI)", pp. 235-244, 2002.

[4] D. Bielser and M. H. Gross, "Interactive Simulation of Surgical Cuts", Proc. Pacific Graphics, pp.116-125, 2000.

[5] F. Ganovelli and P. Cignoni and C. Montani and R. Scopigno, "Enabling Cuts on Multiresolution Representation", The Visual Computer (Springer), Vol. 17, pp. 274-286, 2001.

[6] H. W. Nienhuys and A. F. van der Stappen. "Combining Finite Element Deformation with Cutting for Surgery Simulations", Proc. Eurographics, pp. 274-277, 2000.

[7] D. Serby and M. Harders and G. Szekely, "A New Approach to Cutting into Finite Element Models", Medical Image Computing and Computer Assisted Intervention(MICCAI), pp. 425-433, 2001.

[8] D. Steinemann, M. Harders, M. Gross, G. Szekel, "Hybrid Cutting of Deformable Solids", IEEE Virtual Reality, pp.35-42, 2006.

[9] R. A. Drebin and L. Carpenter and P. Hanrahan, Volume Rendering, Proc. ACM SIGGRAPH, pp. 65-74, 1988.

[10] C. D. Correa, D. Silver, M. Chen, "Discontinuous Displacement Mapping for Volume Graphics", Proc. Volume Graphics, pp. 9-16, 2006.

[11] B. Cabral, N. Cam and J. Foran, Accelerated Volume Rendering and Tomographic Reconstruction using Texture Mapping Hardware, Proc. Volume Visualization Symposium, pp. 91-98, 1994.

Simulating Lung Tumor Motion for Dynamic Tumor-tracking Irradiation

Megumi Nakao, Ayako Kawashima, Masaki Kokubo and Kotaro Minato

Abstract– **This study proposes methods for the support of radiotherapy planning for dynamic tumor-tracking irradiation for lung tumors. It aims to simulate the deformation of the lung caused by respiration and to visualize the result as DRRs (Digitally Reconstructed Radiographs) in real time. Our lung-deformation model treats the lung as an elastic object and analyzes the deformation based on linear FEM (the Finite Element Method). The simulation models the lung using CT volume data and generates a model with boundary conditions with freely adjustable regions, displacements, and phases. The doctor planning the radiotherapy can reproduce the movement of the lung tumor by freely adjusting the regions, displacements, and phases of the boundary conditions while comparing the position of the lung tumor in an X-ray photograph. For high-speed display we propose a method for rapid-generation DRRs by slice-based volume rendering. The result of several functional evaluations and trials of simulation established that the proposed method can describe the movement of the lung tumor with adequate precision. The developed system is expected to be useful for radiotherapy planning for real-time tumor-pursuing irradiation.**

I. Introduction

Radiotherapy is regarded as popular, efficient, less-invasive treatment for cancer. The main challenges in radiotherapy are to preserve as many normal cells as possible by irradiating at only limited volumes around the tumor, and to reduce harmful side effects by administering the minimum effective dose. In the case of a lung cancer, however, the perpetual movement of the tumor as the lungs respire makes it difficult to irradiate around the tumor[1][2]. This necessitates the continuous recalculation of the irradiation field to capture the position of the tumor as it moves.

Our aim was to establish continuous, dynamic tumor-tracking irradiation without any additional loads to patients. **Fig. 1** shows the radiation therapy system being developed at the Foundation for Biomedical Research and Innovation. This system is capable of swinging the irradiation head according to the gimbals mechanism. If the movement of the lung tumor is accurately predictable or estimated, continuous tumor-tracking irradiation while pursuing the lung tumor can be performed. This approach shortens radiation time as well as avoids radiation of normal cells.

Success in continuous tumor-tracking irradiation requires accurate estimation of 3D position and shape of the lung tumor during irradiation. Time-series X-ray radiographs can be acquired during treatment. However, as the images do not always give clear information around tumor due to the characteristic of X-ray imaging, radiologists generally use CT volume data for the radiotherapy planning. Moreover, in order to reconstruct time-varying 3D position and shape of the tumor, only 2D image data and its processing are not sufficient.

This study proposes a method to support radiotherapy planning for dynamic tumor-tracking irradiation for lung tumors. Our method simulates the deformation of a lung caused by respiration and displays the result at high-speed as DRRs (Digitally Reconstructed Radiographs). The lung-deformation simulation treats the lung as an elastic object and analyzes the deformation of the organ by FEM (the finite element method).

II. Dynamic Tumor-tracking Irradiation

Fig. 2 shows the outline of the proposed dynamic tumor-tracking irradiation. Two types of data can be obtained before the treatment begins: CT volume data taken at a respiratory standstill and continuous time series X-ray photographs. The next step is to simulate the lung deformation by FEM using CT volume data. This analysis uses lung-shaped tetrahedral grids and treats the lung as an elastic object. The simulation target is lung deformation and movement of tumor caused by respiration. The simulation results are displayed as DRR for an assessment of their accuracy in comparison with the continuous time series X-ray photographs. If the accuracy cannot be verified, the surgeon can change the simulation parameters and retry a simulation to re-create the movement of the lung tumor along with respiration.

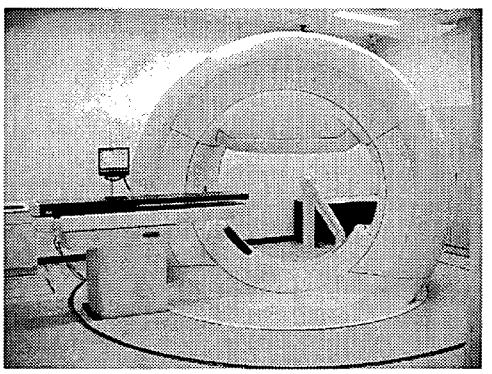

Fig. 1 A new radiation therapy system allowing swing of theirradiation head in real time.

Megumi Nakao, Ayako Kawashima and Kotaro Minato are with the Nara Institute of Science and Technology, Nara, JAPAN {Telephone: +81-743-72-5179, E-mail: meg@is.naist.jp}

Masaki Kokubo is with Institute of Biomedical Research and Innovation, Kobe, JAPAN.

1-4244-0923-3/07/$25.00 ©2007 IEEE.

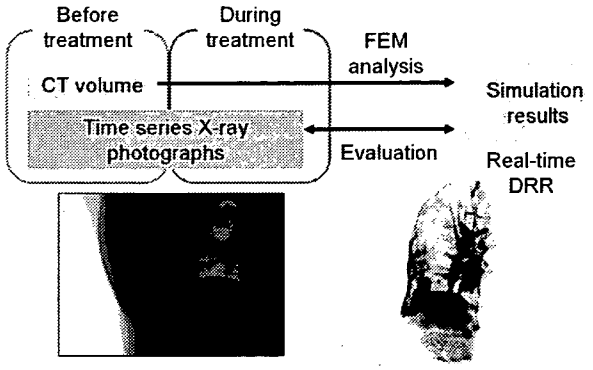

Fig. 2 A basic flow of dynamic tumor-tracking irradiation. 3D position of the tumor is estimated by finite element lung model. The simulation results are visualized as DRRs and evaluated with X-ray photographs.

III. Displacement Estimation of Lung Tumor

Respiration involves two major processes: inspiration and expiration. During inspiration, the inspiratory muscles contract, the diaphragm descends, and the rib cage rises. As the volume of the thoracic cavity increases, air flows into the lungs. During expiration, the inspiratory muscles relax, the diaphragm rises, and the rib cage descends. As the volume of thoracic cavity decreases, the lungs deflate, releasing an outflow of air. As a first step to lung deformation analysis, we regarded the lung as an elastic object and simulate its dynamic behavior using FEM.

We use CT volume data to describe the 3D shape of the lung. For estimating displacement of the lung tumor, we model the lung as an elastic object and simulate its dynamic behavior using FEM. **Fig. 3** shows the developed lung model with boundary conditions. The tetrahedral mesh was created from patient CT dataset. We categorized all vertices $\mathbf{V} = (\mathbf{v}_1, \mathbf{v}_2, \ldots, \mathbf{v})$ into four groups $\mathbf{V}_r$, $\mathbf{V}_d$, $\mathbf{V}_t$ and $\mathbf{V}_b$ like in **Fig. 4**, and defined boundary conditions on the vertices to solve FEM formulation.

$$\mathbf{V} \longrightarrow \begin{cases} \bullet \text{ Rib cage vertices: } \mathbf{V}_r \\ \bullet \text{ Diaphragm vertices: } \mathbf{V}_d \\ \bullet \text{ Trachea vertices: } \mathbf{V}_t \\ \bullet \text{ Rib cage(back) vertices: } \mathbf{V}_b \end{cases}$$

The trachea vertices are set to remain in a fixed position, that is, unaffected by the respiratory movement. The vertices on the diaphragm and rib cage are updated based on the formula (1) and (2) respectively. The movement of rib cage back vertices are constrained for one direction. The vertices around the rib cage do not move downward toward the couch

$$\Delta \mathbf{v}_i = a_r \sin 2\pi f(t + w_r)\mathbf{n}_i \quad (1)$$

$$\Delta \mathbf{v}_j = a_d \sin 2\pi f(t + w_d)\mathbf{n}_j \quad (2)$$

IV. Texture-based DRR Generation

We also developed a method (named Texture-based DRR) to create DRRs in real time. We extended the texture-based volume rendering [3] and visualize FEM simulation results as deformable DRRs. Texture-based DRR can be generated by perspective projection of sections with CT textures (proxy geometries) which are defined from tetrahedral mesh. When the vertices of the mesh are displaced by model deformation, the proxy geometries are updated, and the initial grid coordinates are used to map the 3D texture. The voxel values in each tetrahedral element are correctly mapped on the newly created proxy polygons, thereby visualizing the deformed image volumetrically as DRRs.

V. Experiments and Results

The 3D shape of the lung was obtained from CT and its elasticity was empirically set by Young's modulus 0.01 MPa and Poisson's ratio of 0.25. The region around the tumor was modeled by setting Young's modulus at 1.0 MPa. The boundary condition of the diaphragm was set as a phase of 0.6 seconds. One respiratory cycle is set at 3.6 seconds, to keep the same cycle with continuous time series X-ray photographs.

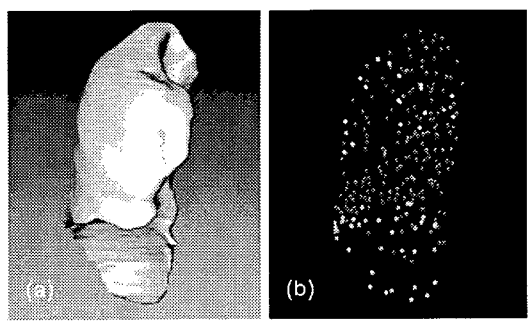

Fig. 3 A lung tetrahedral grid constructed from patient CT dataset. (a) polygonal representation and (b) boundary condition set to the vertices.

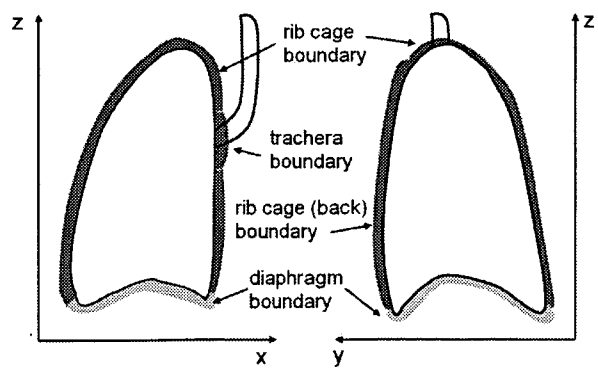

Fig. 4 Boundary condition scheme on the FE lung model for estimating 3D movement of tumor.

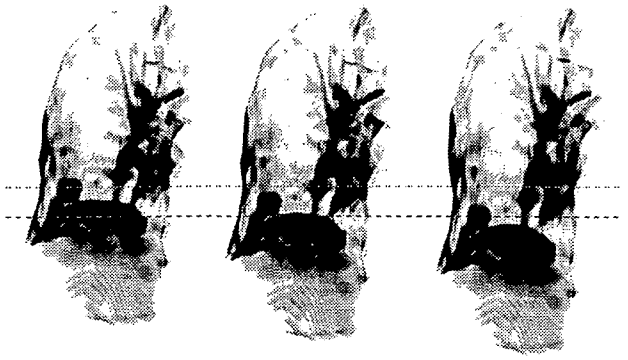

Fig. 5 DRR of simulation results. The movement of tumor is estimated through the FE lung model.

Each boundary condition was set by properly referring to X-ray photographs. **Fig. 5** shows the simulated movement of the lung tumor on time-series DRRs.

We analyzed simulation results of 3D tumor movement. The graph in **Fig. 6** shows tumor position error between time-series X-ray radiographs and simulated tumor position on DRRs. We confirmed the deformation was simulated with very high accuracy in this clinical case (Error within **2 mm**) The irradiation field with our tumor tracking irradiation assumes **48%** of the volume in the conventional methods without tumor tracking.

Lastly, **Fig. 7** demonstrates superimposed deformed DRRs on X-ray radiographs. As the tumor position can be correctly identified with the CT volume data, this visualization will also be useful for recognizing tumor position and shape.

VI. Conclusion

Radiotherapy has become an efficient noninvasive therapy in recent years. In the therapy for lung tumors, however, the mechanism behind the movement of the tumor as the lungs respire has yet to be solved. If the radiotherapy accurately pursues the lung tumor, the technique is certain to advance far from its present state. This research focused on the re-created movement of a lung tumor in one clinical case. This research model is expected to be useful for improving, inspecting, and ultimately realizing the technique of real-time tumor-pursuing irradiation.

Acknowledgment

This research is supported by Grant-in-Aid for Scientific Research (S) (16100001) and Young Scientists (A) (16680024) from The Ministry of Education, Culture, Sports, Science and Technology, Japan.

References

[1] Y. Negoro, Y. Nagata, T. Aoki, T. Mizowaki , N. Araki and K. Takayama, "The effectiveness of an immobilization device in conformal radiotherapy for lung tumor: reduction of respiratory tumor movement and evaluation of the daily setup accuracy", Int. J. Radiat. Oncol. Biol. Phys., Vol. 50, No. 4, pp. 889-898, 2001.

[2] H. Shirato, S. Shimizu and K. Kitamura, "Four-dimensional treatment planning and fluoroscopic real-time tumor tracking radiotherapy for moving tumor", Int. J. Radiat. Oncol. Biol. Phys., Vol. 48, No.2, pp. 435-442, 2000.

[3] B. Cabral, N. Cam, and J. Foran, "Accelerated volume rendering and tomographic reconstruction using texture mapping hardware", ACM Symposium on Volume Visualization, pp. 91-98, 1994.

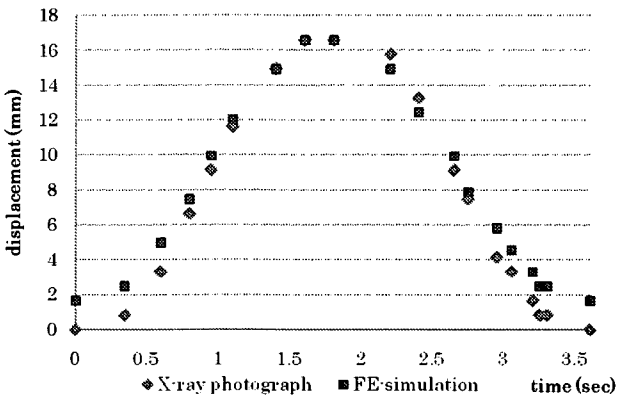

Fig. 6 Displacement of the lung tumor (a) in X-ray photographs and (b) in DRRs generated from FE lung simulation results.

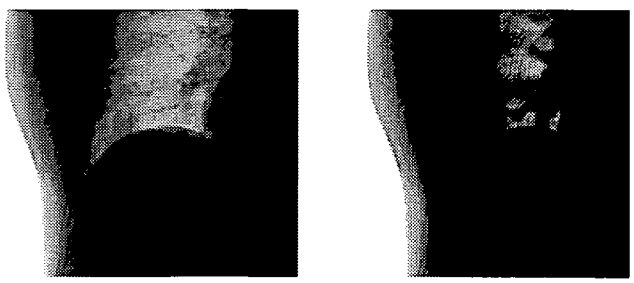

Fig. 7 Superimposing simulation results on time-series X-ray radiographs. This overlay representation supports recognition of tumor's position and shape.

Medicine Meets Virtual Reality 16
J.D. Westwood et al. (Eds.)
IOS Press, 2008

Haptic Rate for Surgical Manipulations with Fingers and Instruments

Yoshihiro KURODA [a,1], Megumi NAKAO [b], Tomohiro KURODA [a], Osamu OSHIRO [a]
[a] *Graduate School of Engineering Science, Osaka University*
[b] *Nara Institute of Science and Technology*

Abstract. In surgery, many kinds of manipulations are conducted using multiple fingers and instruments. The aim of this study is to investigate required haptic rate for multi-finger manipulation and instrumental manipulation. This paper investigated required haptic rate for multi-finger haptic interaction with haptic device and soft tissue deformation. Results of experiment clarified the fact that there is difference of threshold of haptic rate between the number of manipulating fingers.

Keywords. Haptics, Surgical manipulation, Perception

1. Introduction

Growth of computational power has allowed realistic surgical simulation with physics-based deformation, visual/audio effects and haptic feedback. However, 1000Hz of haptic update rate is still a severe requirement, because endless demand for more accurate and realistic simulation increases computational cost. Quality of the simulation has been decreased for keeping the simulation stable.

Psychophysical study has investigated requirements of haptic rate, basically assuming one finger interaction with an object in the case of passive touch [1]. Active touch is psychophysically different from passive touch [2]. On the other hand, in surgery, multiple fingers are used for touching organs or manipulating instruments in the manner of active touch. There are few studies of active touch with multiple fingers. So far, there is no answer to even a simple question "is there any difference of required haptic rate in manipulation using one finger and two fingers".

The aim of this study is to investigate required haptic rate for multi-finger manipulation in the case of active touch. From the understanding of the haptic rate, optimal assignment of computational resource for surgical simulation becomes possible .

[1]Corresponding Author: Graduate School of Engineering Science, Osaka University, 1-3 Machikaneyama-cho, Toyonaka, Osaka, Japan; E-mail: ykuroda@bpe.es.osaka-u.ac.jp

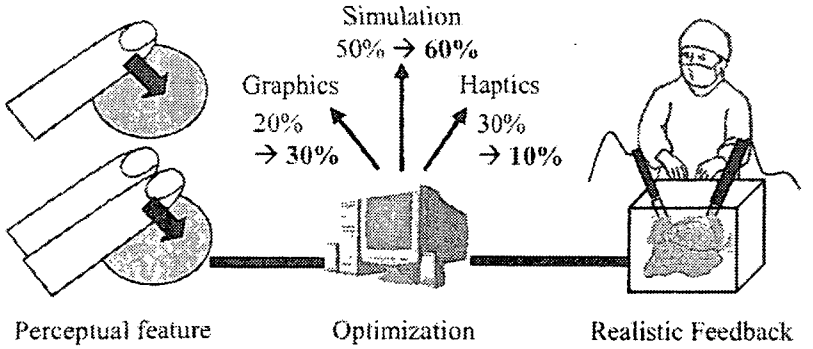

Figure 1. Concept of perception based optimization of physics-based interactive simulation with haptic feedback.

2. Concept

Figure 1 shows a concept of this study. Perception based optimization of physics-based interactive simulation with haptic feedback. Simulation and other functions are able to utilize more computational resource instead of haptics.

If haptic rate is high enough, a user perceives continuous force. However, if not, a user perceives discontinuous force like vibration on fingertip. This causes unrealistic sensation because of insufficient haptic rate. In this study, a threshold of haptic rate which makes a user feel vibration is investigated. Thus, haptic rate must be examined while a user moves their fingers or instrument actively.

3. Experiments and Results

We developed a system which controls haptic rate freely and records user's manipulation during a task. Multi-fingered and endoscopic instrument typed haptic devices CyberForce™ and Xitact IHP™ were equipped. A plate object (20cm x 20cm x 1.5cm in size) object consists of 1334 vertices and 4745 tetrahedron (0.2MPa Young's modulus and 0.4 Poisson's ratio). Linear finite element method was implemented for soft tissue modeling.

A hypothesis in this experiment was "a person is less sensitive to discrete changes in force feedback, perceived as step changes in force or vibration, when performing multi-finger manipulation and instrumental manipulation with an elastic object". 9 volunteer students participated in the experiment. 750 patterns of update rate e.g. 100Hz, 83Hz, 56Hz, 42Hz, 33Hz, 28Hz, 24Hz, 21Hz, 19Hz, 17Hz, 15Hz, 14Hz, etc. were prepared.

A subject pushed a plate object with designated fingers and answers if he/she feels displayed force as continuous force or vibration, until a threshold of haptic rate to feel vibration is found. For standardizing a manipulation, a subject was told to exert forces from 0.5N up to 1.0N by pushing manipulation. Pushed area was colored blue when the exerted force was around 0.5N and colored red around 1.0N, as shown in Figure 2(left).

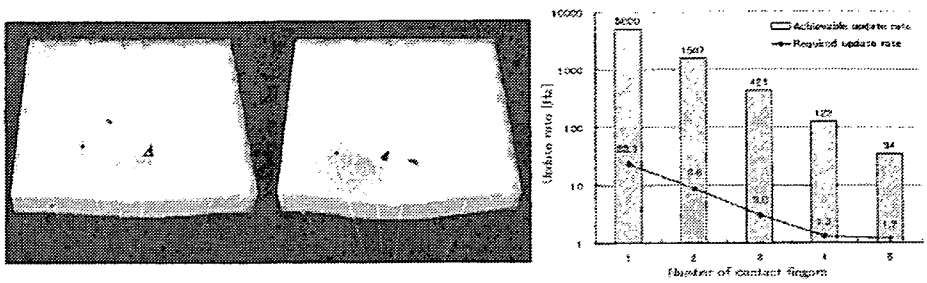

Figure 2. (left) A subject pushes elastic object with one and two fingers
(right) Balance of increase and decrease of haptic update rate with multiple fingers

Average thresholds of haptic update rate in the case of one to five fingers were 23.3, 8.8, 3.0, 1.3 and 1.2 Hz, respectively. Statistical differences by t-test ($p<0.05$) were found in average thresholds between one and two fingers, and also between two and three fingers. The result supported the above hypothesis.

4. Discussions and Conclusion

In this experiment, only haptic rate for pushing manipulation was investigated. More update rate would be required in stroking manipulation, because rapid change of force direction stimulate another receptors. However, this experiment clarified the fact that there is difference of threshold of haptic rate between the number of manipulation fingers.

This paper examined required haptic rate for multi-finger haptic interaction. The result of this study allows assigning excess computational resource to other functions in surgical simulation. Figure 2(right) shows relationships between achieved update rate on PC and required rate with the number of contact fingers. The graph shows that the increase and decrease of the rates with the number of fingers balance.

Acknowledgements

This research was partly supported by Grant-in-Aid for Scientific (S16100001) and Exploratory Research (18659148) from JSPS, and Grant-in-Aid (H18-Medicine-General-032).

References

[1] M. Minsky, M. Ouh-young, O. Steele, F. P. Brooks, Jr., and M. Behensky, "Feeling and seeing: Issues in force display", *Symposium on Interactive 3D Graphics*, (1990), 235-243.
[2] J. Gibson, "Observations on active touch", *Psychological Review* **69(6)** (1962), 477-491.

Construction of Training Environment for Surgical Exclusion with a Basic Study of Multi-finger Haptic Interaction

Yoshihiro Kuroda[1] Makoto Hirai[2] Megumi Nakao[3] Toshihiko Sato[4]
Tomohiro Kuroda[5] Yasushi Masuda[1] Osamu Oshiro[1]
[1]*Graduate School of Engineering Science, Osaka University, Japan*
[2]*Production Systems Research Laboratory, Kobe Steel, Ltd., Japan*
[3]*Graduate School of Information Science, NAIST, Japan*
[4] *Institute for Frontier Medical Sciences, Kyoto University, Japan*
[5]*Department of Medical Informatics, Kyoto University Hospital, Japan*
E-mail: ykuroda@bpe.es.osaka-u.ac.jp, m-hirai@kobelco.jp, meg@is.naist.jp, tsato@frontier.kyoto-u.ac.jp, tkuroda@kuhp.kyoto-u.ac.jp, ymasuda@bpe.es.osaka-u.ac.jp, oshiro@bpe.es.osaka-u.ac.jp

Abstract

Virtual reality based surgical simulator allows a repetitive training without spoiling patients. Exclusion is an important surgical manipulation of pushing aside organ to make a hidden tissue visible. The authors propose an organ exclusion training simulator with multi-finger haptic interaction and stress visualization. The system equips FEM-based soft tissue deformation and exoskeletal haptic device CyberForce. Real-time simulation was achieved with a prototype system. Results of training trial suggested effectiveness of stress visualization especially in early training days. Subjective evaluation by surgeons cleared its potential. Results of a basic study showed decrease of required refresh rate in multi-finger interaction compared with single finger interaction. It suggested the system can keep realism even if calculation time is increased by multi-finger interaction.

1. Introduction

Repetitive experience is a basic approach to obtain a manual skill, which is strongly related to haptic sensation. In medicine, less and less training opportunity becomes a problem, because animals tend to be forbidden to be sacrificed for training. Residents cannot avoid training their skills with real patients, although it has a risk of damaging them. Organ exclusion is a surgical manipulation of pushing aside organ to make a hidden tissue visible or to enlarge workspace as shown in Fig.1. A surgeon excludes liver with multiple fingers to make a hidden vessel visible. Improper manipulation causes fatal damage of the manipulated tissue.

In this paper, exclusion training simulator with multiple fingers is developed with a basic study of multi-finger haptic interaction with an elastic object.

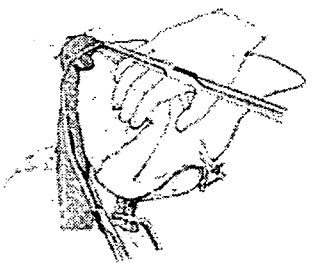

Figure 1. Liver exclusion. A vessel behind liver becomes visible by exclusion with fingers.

2. Background

Virtual reality based surgical simulator has been intensively studied and several simulators are commercially available [1]. Some simulators give an opportunity to know surgical procedures with a specific instrument (e.g. endoscopic forceps). The others provide training environment of a surgical tool (e.g. knife, needle). However, manual training of exclusion, which includes multi-finger haptic interaction, has never been provided. The system should support multiple-finger interaction with an elastic object. Virtual reality system has a strong advantage of showing hidden information in real world

0-7695-2738-8/07 $25.00 © 2007 IEEE

e.g. internal deformation of deformed object or stress concentration. The system will enable efficient surgical training, if physical status of soft tissue can be simulated in real-time and displayed to the user interactively.

Several force feedback devices for multiple fingers have been developed [1, 2, 3]. However, developed applications with multi-finger haptic interaction are very few. One of possible reasons is "refresh rate" problem, especially for displaying high stiffness of rigid wall, which requires high refresh rate (more than 1,000Hz). If an object is softer, a system can provide realistic force sensation with lower refresh rate.

Some studies investigated the requirements of refresh rate for realistic interaction with a virtual stiff wall. Soft tissue has far less stiffness. Psychophysical studies of haptic perception in finger's manipulation have been done intensively. Pang et al. investigated JND (Just Noticeable Difference) of force in squeezing manipulation [4]. Lederman and Klatzky ensured the importance of spatially distributed fingertip force in a palpation-like task [5]. However, difference of perceptual features of haptic interaction with single and multiple fingers is unclear. The condition of used fingers might effect on required refresh rate.

There are many variations of finger manipulations with an elastic object (e.g. pushing, grasping, stroking). In surgical exclusion, a surgeon holds/grasps the object by fingers to control its location and deformation. Cutkosky and Howe categorized grasp into two grasps: power grasp and precise grasp [6]. Power grasp is a manipulation not only with fingertips but also with middle phalanx and a palm for exerting much force on the object. On the other hand, precise grasp is a manipulation only with fingertips for exerting fine force on the object with sensing reaction force at the same time. Surgical exclusion is categorized into precise grasp and then a manipulation with fingertips is significant, because improper manipulation causes fatal damage to organ.

3. Exclusion simulation with multi-finger haptic interaction

3.1. Requirements

Exclusion training system should allow interactive manipulation with realistic force sensation on fingertips. The system of suggesting danger of a manipulation will help understanding a nature of the relationship between manipulation and its effect and help acquiring a skill. If stress exceeds a limit, soft tissue is destructed and loses its function. In exclusion, a manipulation of avoiding stress concentration is an essential skill. Information of stress distribution will be helpful. Although information can be displayed in various manners like visual, haptic and audio display, visual display gives easy understanding of spatial information such like stress distribution.

Therefore, requirements of exclusion training system can be defined as follows.

- Visual display of accurate and interactive soft tissue deformation based on physics
- Haptic display of accurate reaction force
- Visual display of stress distribution based on physics
- Multi-finger haptic interaction with elastic object

3.2. Multi-finger interaction environment

Fig.2 illustrates interaction method of multiple fingers with an elastic object. The method considers passive contact which is arisen by other finger's action to the object. In grasping simulation with a rigid body, a solution of treating passive contact not by processing once but by processing at several steps as active contacts are used. The simulation loop runs very fast (300Hz or more than 1kHz [7]) and then temporary simulation results (invasion of a finger into an object) is not perceivable to users from visual information. On the other hand, simulation with physics-based deformable model can provide realistic haptic sensation with less haptic refresh rate (100Hz or less). In this case, if the procedures are separated to several steps, temporary deformation can be visually perceived by users and lacks realism. In exclusion simulation, both active and passive contacts between a finger and an object are considered.

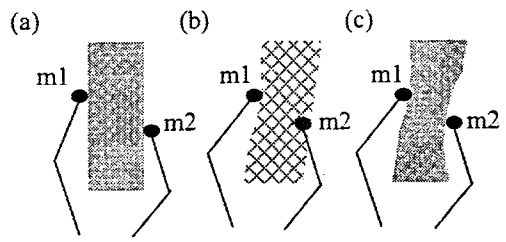

Figure 2. Temporary deformation based multi-finger interaction method with an elastic object. (a) Initial state. (b) Temporary state. The object is deformed by a manipulator (m1). Other manipulator (m2) invades into the object. (c) Contacts by manipulators are considered.

Interactive simulation system with haptic display requires high refresh rate of reaction force and fast calculation of the simulation. In the study of surgical simulation, finite element method (FEM) has been

0-7695-2738-8/07 $25.00 © 2007 IEEE

recognized as one of the most accurate deformation methods. The real-time simulation of non-linear elastic deformation is hard with current CPU power. Hirota proposed a method of real-time calculation of reaction force with linear finite element model [8]. Reaction forces at contact fingers are calculated in real-time.

3.3. Perceptual features of multi-finger haptic interaction

Sufficiency of refresh rate of force feedback provided by a system determines realism of the simulation. However, necessary refresh rate is not clear. Few studies can be found for investigating the difference between single and multi-finger interaction [9]. One question is whether a person requires same refresh rate even in a situation using with multiple fingers or not. In general, in the case of multi-finger interaction, more calculation time for deformation and reaction force is needed compared with single finger interaction. However, if required refresh rate is decreased in multi-finger interaction, increase of computation and decrease of required refresh rate can balance out or at least necessary additional computational resource is changed.

4. Prototype system

As shown in Fig.3(a), the system consists of PC (Intel Xeon 2.6GHz x 2, 1GB memory, RADEON9600 256MB graphic board), display and CyberForce system (CyberForce, CyberGrasp, CyberGlove). Position data is updated at 100Hz. Low refresh rate is enough with low stiff object like soft tissue.

In order to allow various manipulations with multiple fingers in wide workspace, exoskeletal haptic device CyberForce™[1] as shown in Fig.3(b) was used. The device not only gives force sensation on fingertips but also provides force to resist hand movement.

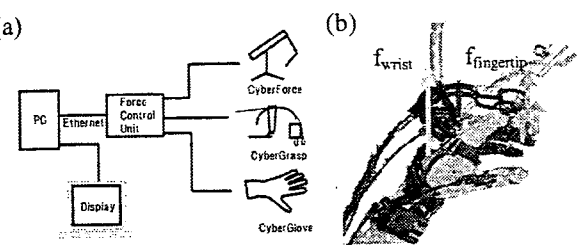

Figure 3. (a) System configuration. (b) Multi-finger haptic device CyberForce. Forces can be displayed to each finger and a wrist.

FEM with linear elasticity and Hirota's method [8] are employed in the system. In order to provide accurate sensation, calculated reaction force with FE model must be displayed to fingers. However, due to device's restriction of freedom of fingertip movement, only tangential component of reaction force is displayed to finger and remaining force is displayed only to wrist. In real world, when a person pushes an object, applied force on a fingertip is conveyed and internal force arises on wrist. However, a mechanism of the device cannot convey the force to wrist. Thus, internal force in wrist is simulated by displaying force on wrist. Sum of calculated reaction forces on fingertips by FE model is displayed on the wrist. The force is same as real world in the ideal situation where great acceleration does not arise in fingers and wrist movement. Displayed forces on a finger and wrist are shown in Equation 5 and 6.

$$\mathbf{f}_{\text{fingertip}}(i) = \mathbf{f}(i)\cos\theta \tag{5}$$

$$\mathbf{f}_{\text{wrist}} = \sum^{5} \mathbf{f}(i) \tag{6}$$

$(i = 1,2,3,4,5)$

where $\mathbf{f}(i)$ is calculated reaction force on a finger by FEM, $\mathbf{f}_{\text{fingertip}}(i)$ is displayed force on fingertip, $\mathbf{f}_{\text{wrist}}$ is displayed force on a wrist.

5. Experiment of perceptual features of multi-finger interaction

An experiment investigates threshold of refresh rate of force perceived as vibration. A hypothesis in this experiment is "a person is less sensitive to discrete changes in force feedback, perceived as step changes in force or vibration, when performing multi-finger interaction with an elastic object".

The experiment was conducted with a developed system described in section 4. A plate object (20cm x 20cm x 1.5cm in size) was set in virtual environment. The object consists of 1334 vertices and 4745 tetrahedron (0.2MPa Young's modulus and 0.4 Poisson's ratio). 7.5% of both left and right sides of the object was fixed in the environment as shown in Fig.4. The rest part of the object deforms by user's manipulation and reaction force is displayed to the user.

Six volunteer students participated in the experiment. A subject pushes a plate object with designated fingers and answers if he/she feels displayed force as continuous force or vibration. If refresh rate is high enough, a subject feels it as continuous force. In contrast, if refresh rate is low, a subject feels it as vibration. A task was to find a threshold of refresh rate to feel vibration.

0-7695-2738-8/07 $25.00 © 2007 IEEE

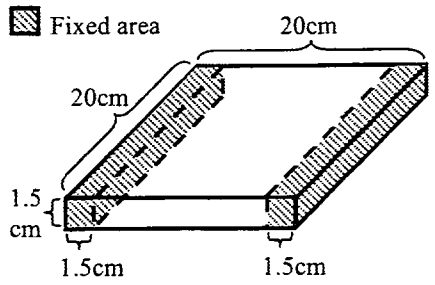

Figure 4. Elastic object used in the experiment.

In order to standardize a condition in each subject, a subject was told to exert 0.5N force on the object first and additionally exert force up to around 1.0N by pushing manipulation, not by stroking manipulation. Visual information helps for a subject to know exerted force, where pushed area was colored blue when the exerted force was around 0.5N and colored red around 1.0N. 250 patterns of refresh rate r (Hz) were prepared by selecting a number i from 1 to 250 as shown in Equation 7. In this equation, a difference of refresh rate can be set smaller in lower rate. This equation was used, because small difference of refresh rate has a great importance in lower refresh rate than in higher rate. If the number i increases, refresh rate decreases like 100Hz, 77Hz, 51Hz, 38Hz, 31Hz, 26Hz, 22Hz, 19Hz, 17Hz, 15Hz...

$$r = \begin{cases} 100 & (i = 1) \\ \dfrac{1}{0.0065 \times i} & (2 \le i < 250) \end{cases} \quad (7)$$

Table 1 shows average thresholds and standard deviations (SD) of refresh rate of force perceived as vibration with single and multi-finger interaction.

Table 1. Threshold of refresh rate in single and multi-finger interaction.

		Refresh rate [Hz] (SD)
Single finger	Index finger	21.3 (35.0)
	Middle finger	14.5 (25.8)
	Third finger	20.8 (33.0)
	Little finger	6.6 (24.9)
Multiple fingers	Index + Middle fingers	4.9 (11.2)
	Middle + Third fingers	3.5 (9.8)

Thresholds ranged from 3.5 to 21.3Hz. If stiff object was used or stroking manipulation was performed, discrete changes would be perceived at higher refresh rate. Statistical difference was found in average thresholds of refresh rate between single and multi-finger interaction by t-test ($p=0.021$). The result supported the above hypothesis. Although statistical difference was not found in the difference of used finger, it was probably because of small samples at each condition.

6. Evaluation of training simulator

6.1. Simulation results

Real-time simulation is essential for virtual reality system with interactive manipulation. Table 2 shows calculation time for reaction force and deformation with 820-noded object, which has cylinder shape and is shown in Fig.6 (a1). Calculation time for reaction force must be sufficient for haptic refresh rate. Deformation time must be below visual refresh rate. Theoretically, calculation time for reaction force increases at $O(3^n)$ according to the number of simultaneous contact fingers. The results approximately showed such an increase of calculation time. Deformation time includes calculation of displacement of all vertices in addition to reaction force calculation. From the results in section 5, as average refresh rates of single and multi-finger interaction was 15.8 and 4.2, respectively, required refresh rates was decreased to approximately one third. Therefore, increase of computational requirements and decrease of required refresh rate by increase of contact fingers are well balanced. Figure 5 shows achieved refresh rate at this system and required refresh rates at multiple contact fingers. Required refresh rates of single and double-finger interaction are derived from the results in section 5 and the rate of more than two contact fingers are estimated by assuming required refresh rate becomes one third by increasing number of contact fingers. The result suggested that realism would be achieved even with many contact fingers.

Fig.6 shows a simulation example of multi-finger haptic interaction with soft tissue models and stress visualization with a vessel. Fig.7 shows stress concentration in the case, where an object has several parts of different stiffness and stress concentration arises around the boundary. The object is modeled as a lung, which has a harder part in the bronchus and pulmonary artery.

0-7695-2738-8/07 $25.00 © 2007 IEEE

Table 2. Calculation time for reaction force and deformation with multiple fingers [msec]

Number of contact fingers	Reaction force	Deformation
1	0.20	1.32
2	0.63	1.95
3	2.36	4.41
4	8.18	12.29
5	29.7	32.36

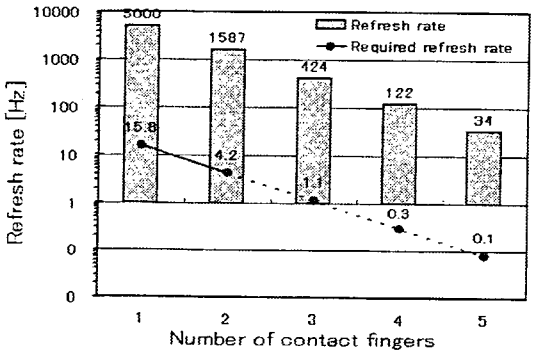

Figure 5. Required and achieved refresh rate of reaction force in multiple contact fingers

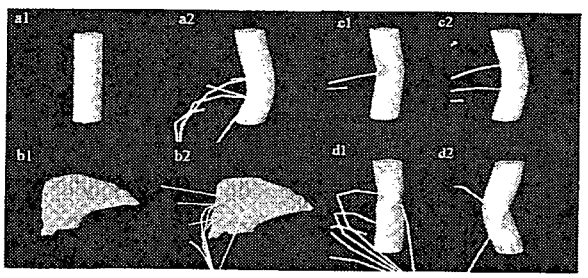

Figure 6. Exclusion simulation of vessel (a1, 2) and liver (b1, 2). Stress distribution caused by different finger numbers (c1,2) and by different finger manipulation (d1,2).

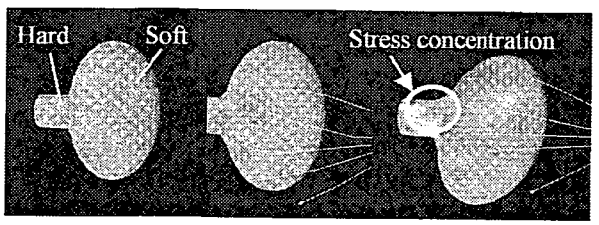

Figure 7. Stress concentration occurred in a simplified lung situation

6.2. Training trial with non-medical persons

The effectiveness of a developed prototype system for exclusion training was examined by training trial. Fig.8 shows two environments of the experiment (object A and B). Each object has features of liver and lung, respectively. Object A has groove like liver, which has several regions and groove can be found in the border. Object B has bronchus and pulmonary artery like lung described in previous subsection. Object A has 0.3MPa Young's modulus (0.4 Poisson's ratio) in the whole body, and object B has 0.1MPa in the soft region and 1.0MPa Young's modulus (0.4 Poisson's ratio) in the hard region in Fig.8. A task was to push aside a target object until a hidden line behind the object is kept visible for a second. 13 volunteers performed 30minutes training in each day for 5days. Stress visualization is provided to group1 (7 persons) and not to group2 (6 persons). A subject was told that he/she tried performing a task with less maximum stress value. 3minutes training and a test without stress visualization was performed in each day.

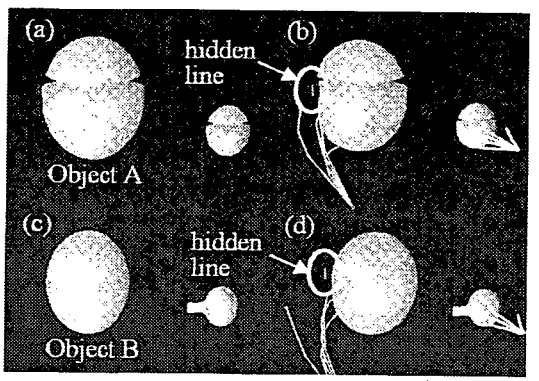

Figure 8. Two environments of training trial. Left side is a front view and right side is a side view. To make a hidden line behind the object visible is a task.

Fig.9 and 10 shows results of the experiment. The result of training trial with object A showed that a learning effect is higher than without displaying stress distribution especially during first two days. The result with object B showed that maximum stress went down in both groups with an exception of the second day, which has higher stress than in first day. This might be why the place of stress concentration in the object B was clear if stress was visible.

0-7695-2738-8/07 $25.00 © 2007 IEEE

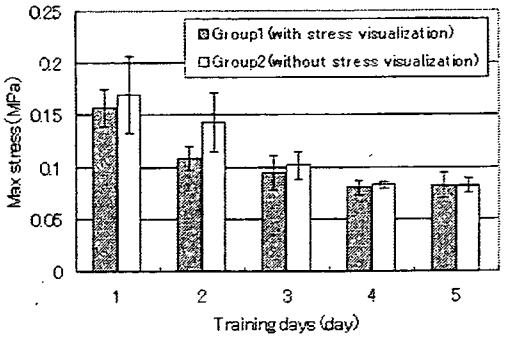

Figure 9. Result of training with object A

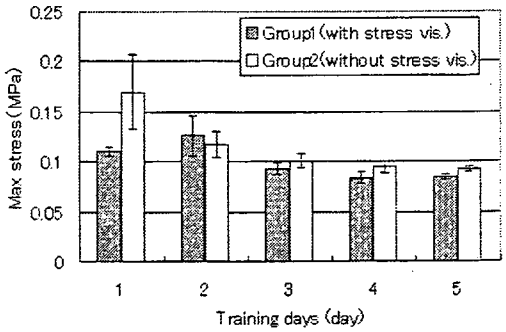

Figure 10. Result of training with object B

6.3. Subjective evaluation by medical doctors

Three surgeons evaluated developed exclusion simulator. The system configuration was described in section 4. Obtained answer was 5 point scale (-2,-1,0,+1,+2) with a questionnaire. Questions and average scores were as follows.

1. The system provides haptic sensation of organ. (avg. score: +1.3)
2. The system is useful for training of organ exclusion. (avg. score: +1.7)
3. Stress visualization is beneficial (avg. score: +1.7)

Results of the questionnaire showed high evaluation of the system in effectiveness for training by surgeons with some room for improvement.

Comments for haptic sensation of organ manipulation:

- The organ gives three-dimensional existence and stiffness is similar with real liver
- Manipulation is not perfectly supported, because organ can be touched only with fingertips.

Comments for effectiveness for training use:

- Exclusion of aorta and great vein is done in digestive surgery in addition to liver. Palm is used sometimes in liver exclusion.
- Considerably effective. Perfectly suit for OSCE (Objective Structured Clinical Examination) of medical student and training of residents

7. Conclusion

This paper proposed an organ exclusion training simulator with a basic study of multi-finger haptic interaction. The results of experiments and subjective evaluation by surgeons suggested that the system was effective for exclusion training especially in early training days. Results of other experiment showed decrease of required refresh rate in multi-finger haptic interaction. Clinical trial with residents is a future work of the training system. Further studies are needed for analyzing multi-finger haptic interaction.

Acknowledgement

This research was partly supported by Grant-in-Aid for Scientific Research (S16100001) and Exploratory Research (18659148) from JSPS, The Ministry of Education, Culture, Sports, Science and Technology, Japan, and Grant-in-Aid (H18-Medicine-General-032), and Nakajima and Kurata Funds, Japan.

References

[1] Immersion, www.immersion.com

[2] D. Gomez, G. Burdea, and N. Langrana, "Integration of the Rutgers Master II in a Virtual Reality Simulation", *IEEE Virtual Reality Annual International Symposium (VRAIS)*, pp.198-202, 1995.

[3] J. Murayama, Y. LUO, K. Akahane, S. Hasegawa, and M. Sato, "A haptic interface for two-handed 6DOF manipulation–SPIDAR - G&G system", *IEICE Trans. on Infomation and Systems*, Vol.E87-D, No.6, 2004.

[4] X. Pang, H. Tan, and N. Durlach, "Manual discrimination of force using active finger motion," *Perception & Psychophysics*, Vol. 49, No. 6, pp. 531-540, 1991.

[5] S. Lederman and R. Klatzky, "Sensing and Displaying Spatially Distributed Fingertip Forces in Haptic Interfaces for Teleoperator and Virtual Environment Systems", *Presence*, 8(1), pp.86-103, 1999.

[6] M. Cutkosky and R. Howe, "Human Grasp Choice and Robotic Grasp Analysis", *Dextrous Robot Hands*, Springer Verlag, New York, pp.68-75, 1990.

[7] G. Burdea and P. Coiffet, *Virtual Reality Technology*, Wiley Interscience, 2003.

[8] K. Hirota and T. Kaneko, "Haptic Representation of Elastic Objects", *MIT Presence*, 2001, 10(5), pp.525-536

[9] A. Maciel, S. Sarni, O. Buchwalder, R. Boulic, D. Thalmann, "Multi-Finger Haptic Rendering of Deformable Objects", In. Tenth Eurographics Symposium on Virtual Environments, p.105-111, 2004.

0-7695-2738-8/07 $25.00 © 2007 IEEE

デジタル・フォレンジックを取り入れた手術動画像生体情報同時記録システムの開発

和田 則仁[1)] 古川 俊治[2)] 森川 康英[3)] 北島 政樹[1)]

慶應義塾大学医学部一般・消化器外科[1)] 慶應義塾大学法科大学院[2)] 慶應義塾大学医学部小児外科[3)]

Development of video recording system for surgical procedure under the concept of digital forensics.

Wada Norihito[1)] Furukawa Toshiharu[2)] Morikawa Yasuhide[3)] Kitajima Masaki[1)]

Department of Surgery, School of Medicine, Keio University[1)] Keio Law School[2)] Department of Pediatric Surgery, School of Medicine, Keio University[3)]

Abstract: Recently, increase in the conflict related to medical practice leads to demands for retrospective inspection of the past medical procedures. Medical practitioners are required to prepare the precise medical record in the legally reliable form in order to demonstrate their own innocence. In the field of endoscopic surgery, all the endoscopic procedure should be continuously recorded throughout the surgery because they require high levels of surgical technique and would be a cause of legal action. Despite the recording with normal video tape is easily altered, technology in digital forensics serves as useful tool against deception in any medical records, especially of surgical procedures. In this study, we established a recording system for digital forensics, which is suitable for routine archive of endoscopic surgery. In this system, patient's data, such as blood pressure and SpO2, and time stump are simultaneously recorded. In order to confirm the quality of recorded information, we used the movie of endoscopic mucosal resection (EMR) for early gastric cancer and laparoscopic surgery for gastrointestinal diseases. For the laparoscopic surgery, MPEG2 (4M) specification is sufficient for retrospective analysis. In the EMR, however, detailed mucosal patterns are carefully examined, non-compressed movie are necessary. Consensus and guidelines related to the digital forensics in medical fields are needed to provide some solution for conflicts in medical malpractices.

Keywords: Digital Forensics, Endoscopic surgery, Video recording

1. はじめに

近年、医療事故が社会的問題化するなか、医療行為を事後的に検証する必要性が増大してきている。医療者は自らの民事および刑事的責任を回避するために、証拠能力の高い形式での医療行為の記録を保存し、自らの医療行為が医療水準に適合した適切なものであったことを証明することが求められる場面が今後増えると予想される[1)]。

特に内視鏡的治療および内視鏡外科手術は、高度な技術を要する局面が多くその適否が紛争の対象になりうるため、手術映像をルーチンに記録することが望ましいと考えられる。これまで映像は通常のビデオテープに録画されることが一般的であったが、これは改竄可能なものであるため法的紛争・訴訟において必ずしも高い証拠性をもつものではない。

我々は訴訟上の証拠能力を高めるため、デジタル情報の改ざん・毀損等の有無を検出可能とするデジタル・フォレンジックの技術を導入して、事後的な検証が可能な水準の画質で手術映像を患者生体情報と同期して記録するシステムを開発した。

2. 対象と方法

対象症例は2006年5月から8月に、慶應義塾大学病院にて内視鏡治療または腹腔鏡手術を受けた患者である。患者には書面で同意を取得した。

方法は、まず前臨床検討として録画済みの映像を種々の方式で圧縮し、記録内容が適正に事後的に検証可能かどうか判定した。判定は2人の内視鏡外科医が独立に行った。

さらに臨床での検討(Fig.1)として、内視鏡治療または腹腔鏡手術の手術用内視鏡映像および室内映像と、血圧、心拍数、酸素飽和度等の生体情報を同期して暗号化処理し、外部のタイムスタンプ局の時刻とともに記録・保存した。非改ざん性を担保するためのトークンは治療の都度取得した(Fig.2)。臨床例として早期胃癌に対する内視鏡的粘膜下切除術および消化器疾患に対する腹腔鏡下手術を用いた。暗号化には、広帯域の動画像でも効率的かつ堅牢に処理しうるストリーム系共通鍵暗号[2)]であるC4S 暗号技術を採用した。臨床評価では、画質・検証可能性の評価以外に、手術室での動作安定性等も検討した。

3. 結果

前臨床で検証可能な画質を評価したところ、腹腔鏡手術症例ではMPEG2 (4M) による圧縮でも手術操作の適切性は検証可能であった。しかし内視鏡的粘膜切除術では早期胃癌を取り扱うため病変の範囲を診断する上で微細な粘膜模様を見極める必要があり非圧縮映像が適切と考えられた。ただし治療デバイスによる操作の検証は、MPEG2 (4M) による圧縮でも可能であった。

臨床での評価について、まず外部時間へのアクセスとして院内のネットワークを利用した場合、ポートの制限などにより安定して接続し得なかったため、PHSに

よる無線でのアクセスを行うことで支障なく記録しえた。暗号化は有意な遅延なく可能であった。画質の検討では、前臨床評価と同様で、手技の記録としてはMPEG2 (4M) による圧縮においても十分事後的検証か可能であったが、早期胃癌の粘膜模様の評価には非圧縮映像が必須であった。

図1 内視鏡治療における記録システムの臨床応用
右上の室内カメラにより術者の手元の映像が、内視鏡画像および生体情報と同期して記録される。

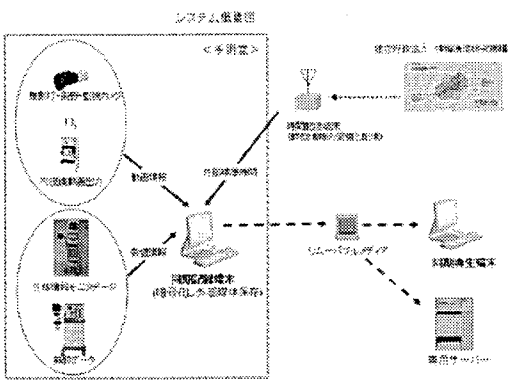

図2 システム構成
手術映像と生体情報が外部時間と同期して記録される。

4. 考察

我々は1999年10月以来、遠隔医療の一環として鏡視下手術における遠隔手術指導システムを実用化してきた[3]。当初はISDN3回線を用いた動画・音声圧縮転送システムを用いていた。しかし、ブロードバンド通信の普及に伴い、安価で質の高い情報が伝送しうる社会的基盤が整備されつつあり、医療の分野でも応用が期待されるようになった。現在、ADSLや家庭用光ファイバー(FTTH)では、ベストエフォートのサービスながら、月々数千円の負担で1～100Mbpsの帯域が得られる。一方でこのような広域ネットワークでは、類型的に要保護性の高い医療情報を扱う上では、高度にセキュリティを確保することが要求される。外科領域における遠隔手術指導では高画質な動画像がリアルタイムで伝送されることが必須の条件となるが、このような大容量の情報を強固に防御するには、従来、高性能のコンピュータを必要としたため実用化が困難であった。そこで暗号強度と通信速度が両立可能な新しい暗号技術により高いセキュリティーを確保しつつ、インターネットを介してリアルタイムに動画像を転送しうるシステムを構築した。これを用いて腹腔鏡補助下幽門側胃切除術(LADG)や内視鏡的胃粘膜切除術(EMR)の遠隔指導を安全に施行しえた。帯域保障のないベストエフォート型のサービスであっても、比較的安定した環境で動作しうるため、今後、広く普及する可能性があると考えられた。

さらに実用的な遠隔手術の形態として、遠隔共同手術システムを開発し臨床応用した[4]。システム構成として、内視鏡はオリンパス社製ImageTrack　を用い、遠隔支援コントローラーは、EndoALPHA　を利用した。デジタル画像伝送装置は富士通ネットワークテクノロジー社製DVSTREAM II　を用いた。通信回線は日本テレコム社のWide-Ether　(70Mbps、外部からアクセスできない閉域網)を利用し、相方向のDVTSで動画像転送を行った。2004年3月25日、49歳、女性の有症状の胆石症患者に対して、腹腔鏡下胆嚢摘出術において遠隔共同手術を行い、安全かつ効果的に内視鏡外科手術を遠隔地の指導医と共同で施行しうることを確認した。

このような外科臨床へのITの応用を進める中で、昨今の社会情勢からフォレンジック性を確保したシステム構築が急務と考えている。

また、医療におけるデジタル・フォレンジックに関してコンセンサスの形成とガイドライン策定が望まれる。

参考文献

[1] 古川俊治.医療事故対応の観点からみたリスクマネジメント—異状死への対応.外科治療 2005;93(3):264-268.
[2] 和田則仁, 古川俊治, 磯部陽, 窪地淳, 北島政樹.Internet protocolによる遠隔医療のための暗号化の強度と速度の検討.日本外科学会雑誌 2004;105:262.
[3] 和田則仁, 古川俊治, 磯部陽, 窪地淳, 北島政樹.消化器疾患の最近の低侵襲治療 遠隔手術.G.I.Research 2004;12:230-234.
[4] 和田則仁.ここまできた遠隔医療—腹腔鏡視野制御を行った遠隔共同手術の臨床応用.新医療 2005;32:122-124.